

## $D_1(2420)$ and its interactions with a kaon: Open charm states with strangeness

Brenda B. Malabarba,<sup>1,2,\*</sup> K. P. Khemchandani,<sup>3,2,†</sup> A. Martínez Torres,<sup>1,2,‡</sup> and E. Oset<sup>2,§</sup>

<sup>1</sup>Universidade de Sao Paulo, Instituto de Física, código postal 05389-970 Sao Paulo, Brazil

<sup>2</sup>Departamento de Física Teórica and IFIC, Centro Mixto Universidad de Valencia-CSIC,

Institutos de Investigación de Paterna, Apartado 22085, 46071 Valencia, Spain

<sup>3</sup>Universidade Federal de São Paulo, código postal 01302-907 São Paulo, Brazil



(Received 16 December 2022; accepted 1 February 2023; published 22 February 2023)

In this work we present an attempt to describe the  $X_1(2900)$  found by the LHCb collaboration, in the experimental data on the invariant mass spectrum of  $D^-K^+$ , as a three-meson molecular state of the  $K\rho\bar{D}$  system. We discuss that the interactions in all the subsystems are attractive in nature, with the  $\rho\bar{D}$  interaction generating  $\bar{D}_1(2420)$  and the  $K\rho$  resonating as  $K_1(1270)$ . We find that the system can form a three-body state but with a mass higher than that of  $X_1(2900)$ . We investigate the  $K\rho D$  system too, finding that the three-body dynamics generates an isoscalar state, which can be related to  $D_{s1}^*(2860)$ , and an exotic isovector state. This latter state has a mass similar to that of the  $X_0(2900)$  and  $X_1(2900)$  states found by LHCb, but a very small width ( $\sim 7.4 \pm 0.9$  MeV) and necessarily requires more than two quarks to describe its properties. We hope that our findings will encourage experimental investigations of the isovector  $K\rho D$  state. Finally, in the pursuit of finding a description for  $X_1(2900)$ , we study the  $\pi\bar{K}^*D^*$  system where  $\bar{K}^*D^*$  forms  $0^+$ ,  $1^+$ , and  $2^+$  states. We do not find a state that can be associated with  $X_1(2900)$ .

DOI: [10.1103/PhysRevD.107.036016](https://doi.org/10.1103/PhysRevD.107.036016)

### I. INTRODUCTION

The motivation of the present work is to find a description for  $X_1(2900)$ , a state with open charm and strange quantum numbers, discovered by LHCb [1,2]. The state was found together with a spin-parity  $0^+$  resonance,  $X_0(2900)$ , in the  $D^-K^+$  invariant mass. We shall refer to these states as  $X_0$  and  $X_1$  in the present paper. Such states clearly require more than two quarks to describe their quantum numbers:  $C = -1, S = 1$ , adding a new task to understanding the nature of the explicitly non  $q\bar{q}$  states found within the last two decades. The masses and widths of the two states are determined in Refs. [1,2] as  $M_{X_0} = 2866 \pm 7$  MeV,  $\Gamma_{X_0} = 57 \pm 13$  MeV,  $M_{X_1} = 2904 \pm 5$  MeV, and  $\Gamma_{X_1} = 110 \pm 12$  MeV. The isospin of the states is not yet well determined, though different suggestions have been brought forward by different model calculations.

A variety of descriptions have also been proposed for the structure of  $X_i$ s, which, naturally, consist of a compact tetraquark structure, or a molecular nature. Most works agree on attributing an isoscalar  $\bar{D}^*K^*$  quasibound state to  $X_0(2900)$  [3–11]. An isoscalar compact tetraquark description has also been tested for  $X_0$  in Refs. [12–16] (as well as for  $X_1$  in Refs. [13,17]), obtaining the mass but not always the width [13] in good agreement with the data [1,2]. Further, a compact tetraquark nature has been disfavored in Ref. [18] for both  $X_0$  and  $X_1$ , on the basis of a relativistic quark model. The authors of Ref. [19] suggest that  $X_0$  and  $X_1$  can be explained as a superposition of a tetraquark and a molecular component. A yet other possibility has been investigated in Ref. [20], indicating that  $X_0$  and  $X_1$  can arise from a triangular singularity in  $\chi_{c1}K^*\bar{D}^*$  and  $D_{sJ}\bar{D}_1K^0$  loops, respectively. In the given scenario, the authors of Refs. [21–23] suggest methods and mechanisms to determine the nature of  $X_i$ s.

From the above discussion, it can be noticed that  $X_0$  has been studied more than  $X_1$ . Since the latter one has spin-parity  $1^-$ , it cannot be contemplated as a  $s$ -wave molecular state of a pair of pseudoscalar/vector mesons. However, one could consider studying a system of an axial and a vector meson interacting in the  $s$  wave, which has indeed been done in Refs. [24–27]. All these former works investigate the  $\bar{D}_1K$  system by writing an effective field for  $\bar{D}_1(2420)$  and relying on the aspects of heavy quark symmetry,

\*brenda@if.usp.br

†kanchan.khemchandani@unifesp.br

‡amartine@if.usp.br

§Eulogio.Oset@if.usp.br

Published by the American Physical Society under the terms of the [Creative Commons Attribution 4.0 International license](https://creativecommons.org/licenses/by/4.0/). Further distribution of this work must maintain attribution to the author(s) and the published article's title, journal citation, and DOI. Funded by SCOAP<sup>3</sup>.

but they find different results. The interactions between  $\bar{D}_1$  and  $K$  have been deduced in Ref. [24] through vector meson exchange diagrams, which is found to be too weak to bind the system. The same formalism is applied to the  $\bar{D}K_1$ ,  $DK_1$ , and  $D_1K$  systems, with  $K_1$  representing  $K_1(1270)$  or  $K_1(1400)$ , but only  $DK_1$  is found to form a bound state. A similar approach is considered in Refs. [25–27] but the results obtained are different. It is concluded in Ref. [25], considering  $\bar{D}K_1$  and  $\bar{D}^*K^*$  as coupled channels, that a large cutoff is required to bind the systems, while the authors of Ref. [26] conclude that, within the uncertainties of their model,  $X_1$  can be interpreted as a  $\bar{D}_1K$  resonance/bound state. Yet another study is reported in Ref. [27], where  $K$  matrices are evaluated with kernels obtained from heavy meson chiral perturbation theory, and an isosinglet,  $\bar{D}_1K$  molecular interpretation is found to be favorable for  $X_1$ , discarding a triangular singularity description.

As a summary, it can be said that though a consensus seems to appear on the description of  $X_0$ , the nature of  $X_1$  is far from clear and further investigations are required. In the present work we investigate a possible explanation for  $X_1$ , in terms of a three-meson bound system:  $K\rho\bar{D}$  (or, equivalently,  $\bar{K}\rho D$ ). We solve three-body equations within the static or fixed center approximation (FCA), considering all interactions in  $s$  wave and considering  $\rho\bar{D}$  to form a cluster. We first solve Bethe-Salpeter equations for the different subsystems, considering appropriate coupled channels, where  $\rho\bar{D}$  and coupled channels generate  $\bar{D}_1(2420)$ ,  $K\rho$  (and the respective coupled channels) generates  $K_1(1270)$ , while  $K\bar{D}$  leads to a weakly attractive amplitude. The  $K\rho$  and  $K\bar{D}$  amplitudes are used as an input to solve the scattering equations for the three-meson system. Our formalism is different to that of Refs. [24–27], since we have the simultaneous treatment of  $\rho\bar{D}$  as  $\bar{D}_1(2420)$  and  $K\rho$  as  $K_1(1270)$  in the system. We investigate different total isospins of the system, and find that a state could arise as a consequence of the interactions in the isoscalar configuration of the  $K\rho\bar{D}$  system. However, the mass of such state would be higher than that determined for  $X_1$  in Refs. [1,2].

Further, we investigate the  $C = S = +1$   $K\rho D$  system too, where the  $KD$  interaction is attractive and forms  $D_s(2317)$ . In this case, we find an isoscalar state, which can be related with  $D_{s1}^*(2860)$ , and an isovector state, which unavoidably requires more than two quarks to describe its properties. The latter exotic state is a  $C = S = +1$  isovector partner of  $X_1(2900)$ .

Finally, inspired by the study in Ref. [4], where bound states of  $\bar{K}^*D^*$  with spin-parity  $0^+$ ,  $1^+$ , and  $2^+$  have been predicted, we investigate if a pion is added to  $\bar{K}^*D^*$ , the resultant three-body system leads to the formation of bound state(s). It is important to mention that the masses obtained for the  $0^+$ ,  $1^+$ , and  $2^+$  states are 2866, 2861, and 2775 MeV, respectively, in Ref. [4], and the  $0^+$  state has

been associated with  $X_0$ . Our special interest lies in verifying if the  $\bar{K}^*D^*$  state with  $J^P = 1^+$  of Ref. [4] together with a pion forms a vector state, which could be interpreted as the  $X_1$  found by LHCb [1,2]. Such a question is motivated by the fact that the masses of  $X_0$  and  $X_1$  differ by less than the mass of a pion. We do not find a clear state formed around 2900 MeV in the  $\pi\bar{K}^*D^*$  system.

The present paper is organized as follows. We first discuss the interactions of  $\rho D$  and coupled channels in detail in the next section, showing that  $D_1(2420)$  is generated from the underlying dynamics. We show that the properties of  $D_1(2420)$  are well described in this model and discuss that meson-meson interactions must give important contributions to explain the nature of this axial state. In the subsequent section, we discuss the formalism used to study the three-body systems and present the results on  $K\rho\bar{D}$  and  $K\rho D$  amplitudes. We dedicate Sec. IV on the discussions of the study of the  $\pi\bar{K}^*D^*$  system. Finally, we present a summary and future perspectives of our present work.

## II. DESCRIPTION OF $D_1(2420)$ IN TERMS OF MESON-MESON INTERACTIONS

The  $D_1(2420)$  meson is listed as the lowest mass charmed axial meson in Ref. [28]. Its mass and width are known with a reasonable precision, with the values  $2422 \pm 0.6$  and  $31.3 \pm 1.9$  MeV, respectively. Interestingly, there exists another axial meson with a very similar nominal mass,  $D_1(2430)$ , but with the width of the order of  $314 \pm 29$  MeV. Keeping this large width in mind, it should be difficult to decide which of the two aforementioned states is the lightest axial with charm, as also discussed in Ref. [29]. Besides, it is important to recall that in spite of having a very similar mass, same quantum numbers, the two states have very different decay widths. The main decay channel of  $D_1(2430)$  is  $\pi D^*$  and due to a large phase space available for the decay, the corresponding decay width turns out to be large. Given the similarity in the masses and quantum numbers of  $D_1(2420)$  and  $D_1(2430)$ , but a large difference between their widths, one can infer that the two states must have a different nature.

Indeed, on the basis of a coupled channel study of pseudoscalar and vector mesons in Ref. [30], it was shown that a state, with the properties like those of  $D_1(2420)$ , arises from the underlying dynamics. It was also found that the state coupled weakly to the  $\pi D^*$  channel, which would explain the small width of  $D_1(2420)$ . However, as we discuss below, the work in Ref. [30] needs to be updated such as to better agree with the experimental data. The formalism in Ref. [30] was built using a Lagrangian based on the  $SU(4)$  symmetry, broken to  $SU(3)$  by suppressing terms in the Lagrangian where the interactions should be driven by the exchange of charmed mesons. Different coupled channels were considered with a total charm  $+1$ , and three poles were found in the complex energy plane when calculating the modulus squared of the two-body  $t$  matrix in  $I = 1/2$ .

The corresponding pole positions [30] are these:  $(2311.24 - i115.68)$ ,  $(2526.47 - 0.08)$ , and  $(2750.22 - i99.91)$  MeV. The authors attempted to identify the pole at  $(2526.47 - 0.08)$  MeV with the state  $D_1(2420)$  in Ref. [30], whose mass and width are  $2422.1 \pm 0.6$  and  $31.3 \pm 1.9$  MeV, respectively [28]. Even when the finite widths of the  $\rho$  and  $K^*$  mesons were considered in Ref. [30], and a width of 26 MeV was obtained for the state identified with  $D_1(2420)$ , the mass remained about 100 MeV above the mass observed experimentally.

In view of the discrepancy between the data and the results presented in Ref. [30], we update the latter model by (1) considering additional diagrams and (2) fine-tuning the parameters of the theory, which are a decay constant present in the potential and a subtraction constant regularizing the divergent loop function in the Bethe-Salpeter equation. We have verified that both the aforementioned corrections are necessary to well describe the properties of  $D_1(2420)$  and any one of the two changes alone is not sufficient.

In the present work we consider box diagrams involving the exchange of pseudoscalar mesons (pions), which were not included in Ref. [30].

As shown in Ref. [31], considering a Lagrangian, like the one used in Ref. [30], is compatible with considering contributions from diagrams with the exchange of a vector meson in the  $t$ -channel, as depicted in Fig. 1, with the vertices determined from the local hidden symmetry Lagrangian of Ref. [32], and taking the limit  $t \rightarrow 0$ . This fact illustrates that box diagrams, involving exchange of pions (as shown in Fig. 2), are an alternative source of contributions to the lowest order pseudoscalar-vector-meson amplitudes, and were not considered in Ref. [30].

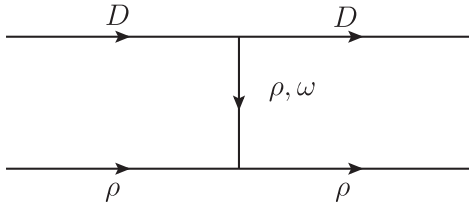


FIG. 1.  $\rho D$  interaction proceeding through the exchange of vector mesons in the  $t$  channel.

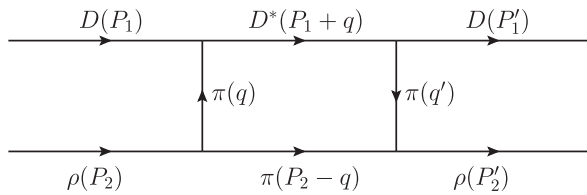


FIG. 2. Box diagrams for the  $\rho D \rightarrow \rho D$  transition in the isospin basis, considering the exchange of pseudoscalar meson,  $\pi$ , in the  $t$  channel.

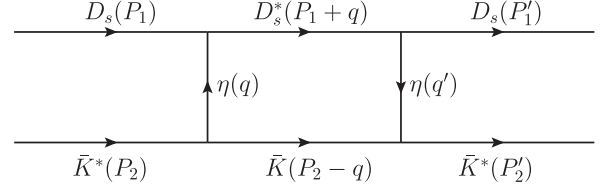


FIG. 3. Box diagrams for the transition  $D_s \bar{K}^* \rightarrow D_s \bar{K}^*$  proceeding through the exchange of pseudoscalar mesons in the  $t$  channel.

Before proceeding further, it is important to mention that the pole associated with  $D_1(2420)$  in Ref. [30] was found to couple strongly to only two channels:  $\rho D$  and  $D_s \bar{K}^*$ . The couplings for the remaining channels were found to be smaller by about a factor of 5 to 10. Thus, we essentially need to consider box diagrams for the  $\rho D$  and  $D_s \bar{K}^*$  channels.

Furthermore,  $D_s \bar{K}^* \rightarrow D_s \bar{K}^*$  scattering, involving pseudoscalar meson exchange, proceeds through the mechanism depicted in Fig. 3. As can be seen, the exchanged ( $\eta$ ) particles involved in the loop, contrary to the corresponding ones in Fig. 2 (pions), are far from being on shell,<sup>1</sup> and they are heavier when compared to those present in the loop shown in Fig. 2. It can be easily verified that the case for the transition between  $\rho D$  and  $K^* \bar{D}_s$  is similar. Consequently, we can say that an important contribution is expected to arise only from the box diagram shown in Fig. 2.

To obtain the amplitude for the diagram in Fig. 2, we need to determine the contributions from each vertex as well as from the four propagators in the loop. In order to proceed, we recall that the mesons  $D$  and  $\rho$  have isospin 1/2 and 1, respectively, and, hence, the  $\rho D$  system can have total isospin 1/2 or 3/2. We are interested in the  $\rho D$  system with total isospin 1/2 (to obtain a dynamically generated state with the quantum numbers of  $D_1(2420)$  [28]), which can be written as

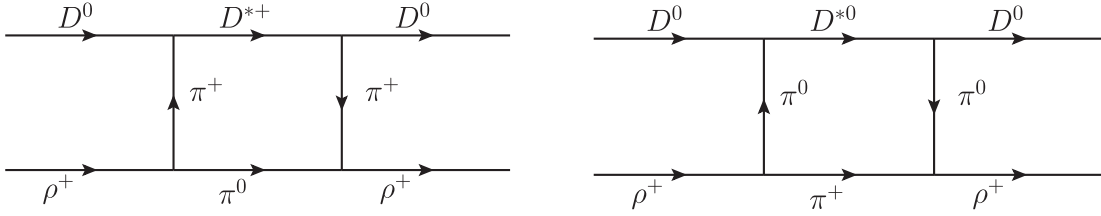
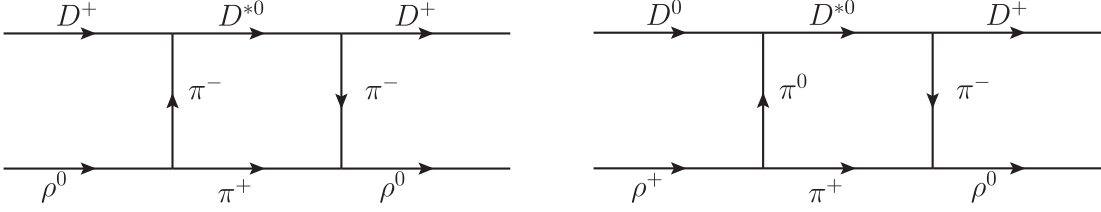
$$|D\rho, I = 1/2, I_3 = 1/2\rangle = -\sqrt{\frac{2}{3}}|D^0\rho^+\rangle + \sqrt{\frac{1}{3}}|D^+\rho^0\rangle, \quad (1)$$

following the phase convention

$$|\rho\rangle = \begin{pmatrix} -|\rho^+\rangle \\ |\rho^0\rangle \\ |\rho^-\rangle \end{pmatrix}, \quad |D\rangle = \begin{pmatrix} |D^+\rangle \\ -|D^0\rangle \end{pmatrix}, \quad |\bar{D}\rangle = \begin{pmatrix} |\bar{D}^0\rangle \\ |D^-\rangle \end{pmatrix}. \quad (2)$$

Using Eq. (1), we can obtain the isospin 1/2 amplitude for  $D\rho \rightarrow D\rho$  as

<sup>1</sup>The threshold  $m_{D_s} + m_\eta$  is around 400 MeV far from  $m_{D_s^*}$ , while  $m_\eta + m_{\bar{K}}$  is about 151 MeV far from  $m_{\bar{K}^*}$ .

FIG. 4. Box diagrams for the transitions  $D^0 \rho^+ \rightarrow D^{*+} \pi^0 \rightarrow D^0 \rho^+$  (left) and  $D^0 \rho^+ \rightarrow D^{*0} \pi^+ \rightarrow D^0 \rho^+$  (right).FIG. 5. Box diagrams for the transitions  $D^+ \rho^0 \rightarrow D^{*0} \pi^+ \rightarrow D^+ \rho^0$  (left) and  $D^0 \rho^+ \rightarrow D^{*0} \pi^+ \rightarrow D^+ \rho^0$  (right).

$$t_{D\rho \rightarrow D\rho}^{I=1/2} = \frac{2}{3} t_{D^0 \rho^+ \rightarrow D^0 \rho^+} + \frac{1}{3} t_{D^+ \rho^0 \rightarrow D^+ \rho^0} - \frac{2\sqrt{2}}{3} t_{D^0 \rho^+ \rightarrow D^+ \rho^0}. \quad (3)$$

As can be seen from Eq. (3), to obtain the  $D\rho \rightarrow D\rho$   $t$  matrix in isospin 1/2 we must determine the amplitudes for the processes:  $D^0 \rho^+ \rightarrow D^0 \rho^+$ ,  $D^+ \rho^0 \rightarrow D^+ \rho^0$ ,  $D^+ \rho^0 \rightarrow D^0 \rho^+$ .

The box diagrams leading to nonzero contributions for the mentioned transitions are shown in Figs. 4 and 5 (with the momenta labels as in Fig. 2).

We use the following vector-pseudoscalar-pseudoscalar (VPP) Lagrangian

$$\mathcal{L}_{VPP} = -ig_{VPP} \langle V_\mu [P, \partial^\mu P] \rangle, \quad (4)$$

to deduce the amplitudes for each of the diagrams presented in Figs. 4 and 5, where the coupling is related to the pion decay constant,  $g_{VPP} = m_\rho / (2f_\pi)$ , with  $f_\pi = 93$  MeV,

$$P = \begin{pmatrix} \frac{\pi^0}{\sqrt{2}} + \frac{\eta}{\sqrt{3}} + \frac{\eta'}{\sqrt{6}} & \pi^+ & K^+ & D^0 \\ \pi^- & -\frac{\pi^0}{\sqrt{2}} + \frac{\eta}{\sqrt{3}} + \frac{\eta'}{\sqrt{6}} & K^0 & D^- \\ K^- & \bar{K}^0 & -\frac{\eta}{\sqrt{3}} + \sqrt{\frac{2}{3}}\eta' & D_s^- \\ D^0 & D^+ & D_s^+ & \eta_c \end{pmatrix}, \quad (5)$$

and

$$V_\mu = \begin{pmatrix} \frac{\rho^0}{\sqrt{2}} + \frac{\omega}{\sqrt{2}} & \rho^+ & K^{*+} & \bar{D}^{*0} \\ \rho^- & -\frac{\rho^0}{\sqrt{2}} + \frac{\omega}{\sqrt{2}} & K^{*0} & D^{*-} \\ K^{*-} & \bar{K}^{*0} & \phi & D_s^{*-} \\ D^{*0} & D^{*+} & D_s^{*+} & J/\psi \end{pmatrix}_\mu \quad (6)$$

Consequently, we get the following common expression for the amplitudes of the diagrams in Figs. 4 and 5

$$-it_{D\rho \rightarrow D\rho}^C = \xi^C \int \frac{d^4 q}{(2\pi)^4} (\vec{\epsilon}_{D^*} \cdot \vec{q})^2 \vec{\epsilon}_\rho \cdot \vec{q} \vec{\epsilon}_\rho \cdot \vec{q} \left( \frac{1}{q^2 - m_\pi^2 + i\epsilon} \right)^2 \frac{1}{(P_2 - q)^2 - m_\pi^2 + i\epsilon} \frac{1}{(P_1 + q)^2 - m_{D^*}^2 + i\epsilon}, \quad (7)$$

where  $\xi^C$  is a coefficient whose values are presented in Table I. It is important to mention here that the expression in Eq. (7) is obtained considering  $\vec{P}_1 = \vec{P}_2 \sim \vec{0}$ , which is a fair approximation at energies close to the threshold of the reaction, as in our case. This latter consideration implies that  $P_1 \sim P_1'$ ,  $P_2 \sim P_2'$ , and consequently  $q = q'$ .

Using Eq. (3), along with the coefficients given in the Table I, we obtain the isospin projected amplitude as

$$-it_{D\rho \rightarrow D\rho}^{box, I=1/2} = 16g^4 \int \frac{d^4 q}{(2\pi)^4} \vec{q} \cdot \vec{\epsilon}_\rho \vec{q} \cdot \vec{\epsilon}_\rho \vec{q} \cdot \vec{\epsilon}_{D^*} \vec{q} \cdot \vec{\epsilon}_{D^*} \left( \frac{1}{q^2 - m_\pi^2 + i\epsilon} \right)^2 \left( \frac{1}{(P_1 + q)^2 - m_{D^*}^2 + i\epsilon} \right) \left( \frac{1}{(P_2 - q)^2 - m_\pi^2 + i\epsilon} \right). \quad (8)$$

The integration over the  $q^0$  variable can be done analytically, by using Cauchy's residue theorem, to get

$$\begin{aligned}
 t_{D\rho \rightarrow D\rho}^{box, I=1/2} &= \frac{16}{3} g^4 \vec{\epsilon}_\rho \cdot \vec{\epsilon}'_\rho \int \frac{d^3 q}{(2\pi)^3} |\vec{q}|^4 F^4(\vec{q}) \left(\frac{M_{D^*}}{M_{K^*}}\right)^2 \frac{1}{2\omega_{D^*}} \left(\frac{1}{2\omega_\pi}\right)^3 \\
 &\times \frac{1}{P_2^0 + P_1^0 - \omega_\pi - \omega_{D^*} + i\epsilon} \left[ -\frac{1}{\omega_\pi} \left( \frac{1}{P_2^0 - 2\omega_\pi + i\epsilon} + \frac{1}{P_1^0 - \omega_\pi - \omega_{D^*} - i\epsilon} \right) \right. \\
 &\left. + \frac{1}{(P_2^0 - 2\omega_\pi - i\epsilon)^2} + \frac{1}{(P_1^0 - \omega_\pi - \omega_{D^*} + i\epsilon)^2} \right] + \mathcal{B},
 \end{aligned} \tag{9}$$

where  $\omega_A = \sqrt{\vec{q}^2 + M_A^2}$ , with  $A = \pi, D^*$  and

$$\mathcal{B} = \frac{16}{3} g^4 \vec{\epsilon}_\rho \cdot \vec{\epsilon}'_\rho \int \frac{d^3 q}{(2\pi)^3} |\vec{q}|^4 F^4(\vec{q}) \left(\frac{M_{D^*}}{M_{K^*}}\right)^2 \frac{1}{2\omega_{D^*}} \left(\frac{1}{2\omega_\pi}\right)^3 \left[ \frac{1}{P_2^0 + 2\omega_\pi} \frac{1}{P_1^0 - \omega_\pi - \omega_{D^*}} \right] \left( \frac{1}{\omega_\pi} + \frac{1}{P_2^0 + 2\omega_\pi} - \frac{1}{P_1^0 - \omega_\pi - \omega_{D^*}} \right). \tag{10}$$

Notice that we have included a form factor in Eq. (9), which we take to be

$$F(q) = \exp\left\{ \frac{(q^0)^2 - \vec{q}^2}{\Lambda^2} \right\}, \tag{11}$$

with  $q^0 = P_1^0 - \omega_{D^*}$ , at each vertex and a factor  $(M_{D^*}/M_{K^*})^2$  to account for the difference between the coupling constants  $g$  for the  $D^* \rightarrow D\pi$  and  $K^* \rightarrow K\pi$  vertices [33]. The value of the cutoff,  $\Lambda$ , is 1200 MeV. The remaining  $d^3 q$  integral is done numerically by setting the upper limit of  $|\vec{q}|$  to 2000 MeV for practical purposes. We have verified that integrating to higher values of  $|\vec{q}|$  does not change the results.

It may be noticed that  $\mathcal{B}$  has no imaginary part because the expression  $(P_2^0 + 2\omega_\pi)^{-1}$  is always positive and  $(P_1^0 - \omega_\pi - \omega_{D^*})^{-1}$  is associated with  $D \rightarrow \pi + D^*$ , a process which does not occur on shell. Due to the mentioned fact, we do not have to worry about these terms having singularities and do not need to include an imaginary part ( $i\epsilon$ ).

The resulting amplitude,  $t_{D\rho \rightarrow D\rho}^{box, I=1/2}$ , is added to the one related to a vector exchange of Ref. [30]. With this new amplitude we solve the Bethe-Salpeter equation, considering coupled channels as in Ref. [30]. Apart from adding

TABLE I. Coefficients  $\xi^C$  present in the expression for the box diagrams in Eq. (7).

Transition	$\xi^C$
$D^0 \rho^+ \rightarrow D^{*0} \pi^+ \rightarrow D^0 \rho^+$	$4g^4$
$D^0 \rho^+ \rightarrow D^{*0} \rho^+ \rightarrow D^+ \rho^0$	$-4\sqrt{2}g^4$
$D^+ \rho^0 \rightarrow D^{*0} \pi^+ \rightarrow D^+ \rho^0$	$8g^4$
$D^0 \rho^+ \rightarrow D^{*+} \pi^0 \rightarrow D^0 \rho^+$	$8g^4$

new diagrams, we have also adjusted the decay constant and the subtraction constant  $\alpha$ , which were set to  $\sqrt{f_{D^*} f_\pi}$  and  $-1.55$ , respectively, in Ref. [30].

Using  $f_\pi$  as the decay constant,  $\alpha = -1.45$ , at the regularization scale  $\mu = 1500$  MeV (which is the same as in Ref. [30]), we find that the modulus squared amplitude for  $D\rho$  in isospin 1/2, spin-parity  $J^P = 1^+$ , peaks at  $\sim 2428$  MeV, with a total width of 33 MeV (see Fig. 6). Our findings are in excellent agreement with the mass and width values determined from the most recent data obtained by the LHCb Collaboration [34],  $M = 2424.8 \pm 0.1 \pm 0.7$  MeV,  $\Gamma = 33.6 \pm 0.3 \pm 2.7$  MeV, and by the BES Collaboration,  $M = 2427.2 \pm 1.0 \pm 1.2$  MeV,  $\Gamma = 23.2 \pm 2.3 \pm 2.3$  MeV [35].

We can, thus, summarize this discussion by mentioning that the addition of the amplitude obtained from the box

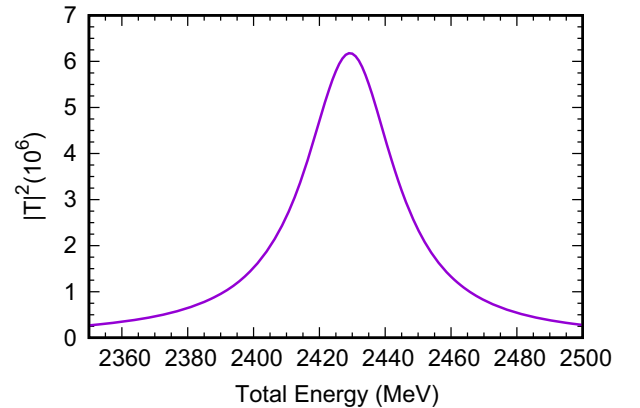


FIG. 6. Modulus squared of the  $D\rho \rightarrow D\rho t$  matrix, in isospin 1/2,  $J^P = 1^+$ . This result is obtained by considering the amplitude of Ref. [30] together with the contribution obtained from the box diagram shown in Fig. 2 and solving the Bethe-Salpeter equation in a coupled channel approach.

diagram increases the width of the state found in Ref. [30] by about  $\sim 7$  MeV. Additionally, the model parameters have been fine-tuned to better describe the properties of  $D_1(2420)$ , like the mass, which now is 2428 MeV instead of the value  $\sim 2526$  MeV found in Ref. [30].

### III. THE $K\rho\bar{D}$ AND $K\rho D$ SYSTEMS

Inspired by the results obtained for the two-body system,  $\rho D$ , and recalling the fact that the  $K\rho$ ,  $KD$ , and  $K\bar{D}$  interactions are attractive in nature, we find it encouraging to explore the systems  $K\rho D$  and  $K\rho\bar{D}$  (the results obtained for the  $D\rho$  system must be equivalent to those for  $\bar{D}\rho$ , given the fact that  $\rho$  is its own antiparticle and a system and its complex conjugate have equivalent descriptions).

To describe the three-body interactions of the  $K\rho D$  and  $K\rho\bar{D}$  systems we solve three-body equations within the static or fixed center approximation [36–38]. The fixed center approximation consists of considering that one of the particles (which is lighter than the other two) interacts with a cluster of the other two strongly interacting particles, which remains unaltered in the scattering. We have a system at hand that is precisely suitable for the aforementioned treatment. The dynamics in the  $K\rho D(K\rho\bar{D})$  system can be described in terms of the interaction of the meson  $K$  with the cluster formed by  $\rho D(\rho\bar{D})$ , which, as shown in the previous section, generates the state  $D_1(2420)$ . In other words,  $D_1(2420)$  can be interpreted as a  $\rho D$  quasibound state. The diagrams contributing to the scattering equations, within such a reorganization of the three-body system, can be drawn as shown in Fig. 7, where the kaon rescatters off the constituents of the cluster.

The three-body  $T$  matrix is obtained by summing two coupled, infinite, scattering series

$$T = T_{31} + T_{32}, \quad (12)$$

with

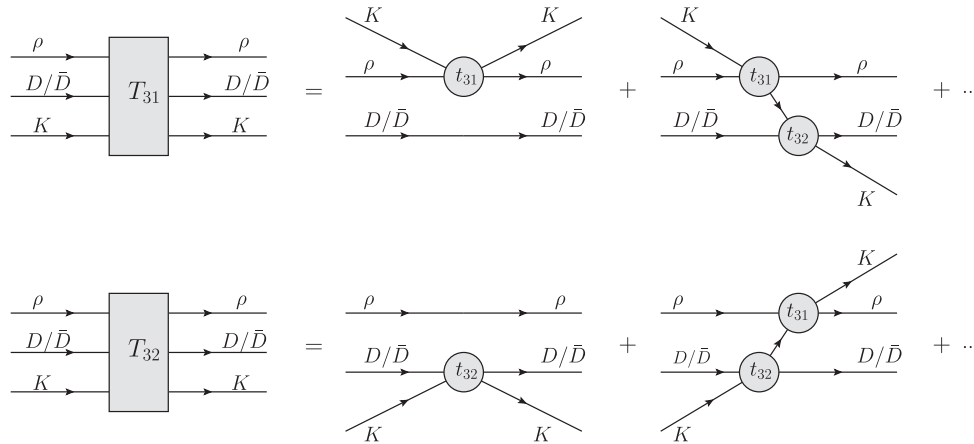


FIG. 7. Diagrams for three-body interactions in the  $K\rho D(K\rho\bar{D})$  system when treating  $\rho\bar{D}(\rho\bar{D})$  as a cluster.

$$T_{31} = t_{31} + t_{31}G_K T_{32}, \quad (13)$$

$$T_{32} = t_{32} + t_{32}G_K T_{31}, \quad (14)$$

where  $t_{3i}$  represent the amplitude of the interaction of the particle labeled as 3 (kaon, in this case) with the  $i$ th particle in the cluster. The function  $G_K$  represents the kaon propagating in the cluster and is given by the following expression [39]:

$$G_K = \int \frac{d^3q}{(2\pi)^3} \frac{F(\vec{q})}{(q^0)^2 - \vec{q}^2 - m_K^2 + ie}, \quad (15)$$

with  $m_K$  being the mass of kaon, and  $q^0$  being the on-shell energy of the kaon in the rest frame of the cluster

$$q^0 = \frac{s - m_K^2 - M_c^2}{2M_c}, \quad (16)$$

where  $M_c$  is the mass of the cluster. In Eq. (15),  $F(\vec{q})$  is a form factor related to the wave function of the constituents of the cluster  $\rho D(\rho\bar{D})$ , and which is introduced to take into account the composite nature of the cluster

$$F(\vec{q}) = \frac{1}{\mathcal{N}} \int_{|\vec{p}|, |\vec{p}-\vec{q}| < \Lambda} d^3\vec{p} f(\vec{p}) f(\vec{p}-\vec{q}), \quad (17)$$

where

$$f(\vec{p}) = \frac{1}{\omega_\rho(\vec{p})\omega_{D(\bar{D})}(\vec{p})} \frac{1}{M_c - \omega_\rho(\vec{p}) - \omega_{D(\bar{D})}(\vec{p})}, \quad (18)$$

with  $\mathcal{N}$  being a normalization factor defined such that  $F(0) = 1$ , and  $\omega_A = \sqrt{m_A^2 + \vec{p}^2}$ , with  $A = D(\bar{D}), \rho$ . The cutoff  $\Lambda$  is taken to be  $\sim 960$  MeV, which is related to the value of the subtraction constant used to regularize the two-body loop functions in the  $D\rho$  and coupled channels

generating  $D_1(2420)$ . We shall vary this value in the range 900–1000 MeV to estimate the model uncertainties.

As shown in the previous section,  $D_1(2420)$  [ $\bar{D}_1(2420)$ ] is generated by the  $\rho D(\rho\bar{D})$  and coupled channel interactions and has a mass  $\sim 2428$  MeV. Hence, we use this value as the mass of the cluster in Eqs. (15) and (18). The  $D_1(2420)$  state also has a finite width, of approximately 33 MeV, which is considered in the formalism by replacing  $M_c \rightarrow M_c - i\frac{\Gamma_c}{2}$  in Eq. (18).

To proceed with the calculations, we need to write the three-body system in a well-defined isospin basis. Within the fixed-center approximation, the three-body

system  $K\rho D$  can be described as an effective two-body  $KD_1(2420)$  system. Since both  $D_1(2420)$  and  $K$  have isospin 1/2, the three-body system can have a total isospin 0 or 1. Considering the sign convention defined in Eq. (2), together with

$$|K\rangle = \begin{pmatrix} |K^+\rangle \\ |K^0\rangle \end{pmatrix}, \quad (19)$$

we can write the  $K\rho D/K\rho\bar{D}$  systems with isospin 0 or 1 as follows:

$$\begin{aligned} |K\rho D, I=0, I_3=0\rangle &= -\frac{1}{\sqrt{6}}|K^+\rho^0 D^0\rangle - \frac{1}{\sqrt{3}}|K^+\rho^- D^+\rangle - \frac{1}{\sqrt{3}}|K^0\rho^+ D^0\rangle + \frac{1}{\sqrt{6}}|K^0\rho^0 D^+\rangle, \\ |K\rho D, I=1, I_3=1\rangle &= \sqrt{\frac{2}{3}}|K^+\rho^+ D^0\rangle - \frac{1}{\sqrt{3}}|K^+\rho^0 D^+\rangle, \\ |K\rho\bar{D}, I=0, I_3=0\rangle &= \frac{1}{\sqrt{6}}|K^+\rho^0 D^-\rangle - \frac{1}{\sqrt{3}}|K^+\rho^- \bar{D}^0\rangle + \frac{1}{\sqrt{3}}|K^0\rho^+ D^-\rangle + \frac{1}{\sqrt{6}}|K^0\rho^0 \bar{D}^0\rangle, \\ |K\rho\bar{D}, I=1, I_3=1\rangle &= -\sqrt{\frac{2}{3}}|K^+\rho^+ D^-\rangle - \frac{1}{\sqrt{3}}|K^+\rho^0 \bar{D}^0\rangle. \end{aligned} \quad (20)$$

However, to calculate the three-body  $T$  matrix within the FCA we must determine the  $t_{31}$  and  $t_{32}$  amplitudes, which describe, respectively, the interaction between a particle, labeled as 3 (in this case the kaon), with the particles, labeled as 1 ( $\rho$ ) and 2 ( $D$ , or  $\bar{D}$ ), of the cluster, respectively. It is then more convenient to use states written in terms of the isospin of the (31) or (32) subsystems. To better explain the isospin dependence, we consider the specific example of total isospin  $I=0$  of the three-body system. For this purpose, we use Clebsch-Gordan coefficients to rewrite the first equation

in the set labeled as Eq. (20) in terms of the isospin of the  $K\rho$  system. We can write, for  $|K^+\rho^0\rangle$ ,

$$\begin{aligned} |K^+\rho^0\rangle &= \left|K, I=\frac{1}{2}, I_3=\frac{1}{2}\right\rangle \otimes |\rho, I=1, I_3=0\rangle, \\ &= \sqrt{\frac{2}{3}}\left|K\rho, I=\frac{3}{2}, I_3=\frac{1}{2}\right\rangle + \frac{1}{\sqrt{3}}\left|K\rho, I=\frac{1}{2}, I_3=\frac{1}{2}\right\rangle, \end{aligned} \quad (21)$$

and similar equations for  $|K^+\rho^-\rangle$ ,  $|K^0\rho^+\rangle$ ,  $|K^0\rho^0\rangle$ . Substituting such expressions in Eq. (20), we find

$$\begin{aligned} |K\rho D, I=0, I_3=0\rangle &= \frac{1}{\sqrt{2}}[|K\rho, I=1/2, I_3=1/2\rangle \otimes |D, I=1/2, I_3=-1/2\rangle \\ &\quad - |K\rho, I=1/2, I_3=-1/2\rangle \otimes |D, I=1/2, I_3=1/2\rangle], \end{aligned} \quad (22)$$

which can be used to determine  $t_{31}$ ,

$$t_{31} = \langle K\rho D, I=0, I_3=0 | t | K\rho D, I=0, I_3=0 \rangle = t_{K\rho}^{1/2}, \quad (23)$$

where  $t_{K\rho}^{1/2}$  is the two-body  $t$  matrix for the  $K\rho$  system in isospin 1/2. For other total isospin values,  $t_{31}$  is a combination of the  $K\rho$  two-body  $t$  matrices in isospin

1/2 and 3/2, with weights determined from products of Clebsch-Gordan coefficients. Similarly, writing  $|K\rho D, I=0, I_3=0\rangle$  in terms of the isospin of the  $KD$  system, we can evaluate  $t_{32}$ , which, in general, can be written in terms of combinations of the  $KD$  two-body  $t$  matrices in isospin 1 and 0. To express this information, we introduce a compact notation by writing

$$t_{31} = \langle K\rho D, I, I_3 | t | K\rho D, I, I_3 \rangle \equiv \vec{\omega}_{31}^I \cdot \vec{t}_{31}, \quad (24)$$

TABLE II.  $\omega_{31}$  and  $\omega_{32}$  for the  $K\rho D(K\rho\bar{D})$  system for total isospin 0 and 1.

Total isospin ( $I$ )	$\vec{\omega}_{31}^I$	$\vec{\omega}_{32}^I$
0	(1,0)	(0,1)
1	(1/9, 8/9)	(1/3, 2/3)

$$t_{32} = \langle K\rho\mathbb{D}, I, I_3 | t | K\rho\mathbb{D}, I, I_3 \rangle \equiv \vec{\omega}_{32}^I \cdot \vec{t}_{32}, \quad (25)$$

where  $\mathbb{D} = D, \bar{D}$  when considering the system  $K\rho D$  or  $K\rho\bar{D}$ , respectively, and  $I$  is the total isospin of the three-body system. The vectors  $\omega_{31(32)}^I$  are the weight factors related to Clebsch-Gordan coefficients, which are summarized in Table II, and  $\vec{t}_{31}$  and  $\vec{t}_{32}$  are defined as follows:

$$\vec{t}_{31} \equiv \begin{pmatrix} t_{K\rho}^{1/2} \\ t_{K\rho}^{3/2} \end{pmatrix} \quad \vec{t}_{32} \equiv \begin{pmatrix} t_{K(D/\bar{D})}^0 \\ t_{K(D/\bar{D})}^1 \end{pmatrix}. \quad (26)$$

It can be noticed that to determine  $t_{31}$  and  $t_{32}$  we need the two-body  $t$  matrices of the  $K\rho$ ,  $KD/K\bar{D}$  systems in the different isospin configurations. These latter amplitudes are obtained by solving Bethe-Salpeter equations, considering all coupled channels relevant in each case, keeping all interactions in the  $s$  wave.

To obtain the two-body  $t$  matrices for the  $K\rho$  and coupled channels we follow Refs. [40,41], where the formalism is built by considering vector mesons as fields transforming homogeneously under the nonlinear realization of chiral symmetry. The model shows that the amplitudes lead to the formation of  $K_1(1270)$ , which is related to two poles in the complex energy plane, and well describes the data on the  $K^-p \rightarrow K^- \pi^+ \pi^- p$  process.

For the  $KD$  ( $K\bar{D}$ ) subsystems and coupled channels we consider as input for the Bethe-Salpeter equation an amplitude obtained from a Lagrangian based on the heavy quark spin symmetry [42]. In this case, the interactions in the charm and strangeness +1 isoscalar system generate  $D_s(2317)$  while the isoscalar  $K\bar{D}$  interaction is found to be weakly attractive in nature. It should be mentioned that the strong relation between the  $KD$  system and  $D_s(2317)$  has been confirmed by analysis of the lattice data too [43–45].

As we have already mentioned, the interactions of the three particles that compose the systems  $K\rho D$  and  $K\rho\bar{D}$  can be interpreted as the interaction of the kaon with a cluster. If we compare the expression for the three-body  $S$  matrix with that for an effective, two-body, kaon-cluster scattering, then we find that in order for both  $S$  matrices to be compatible we must redefine  $G_K$ ,  $t_{31}$ , and  $t_{32}$ , in Eq. (14), as follows [46–48]

$$G_K \rightarrow \frac{1}{2M_c} G_K, \quad t_{31} \rightarrow \frac{M_c}{m_\rho} t_{31}, \quad t_{32} \rightarrow \frac{M_c}{m_{D(\bar{D})}} t_{32}. \quad (27)$$

Having described all inputs necessary for the determination of the three-body  $T$  matrices for the systems  $K\rho D$  and  $K\rho\bar{D}$  in isospin 1 and 0, we are in a position to discuss the results. Let us begin by discussing the results for the  $K\rho\bar{D}$  system, which has the quantum numbers of  $X_1$  ( $J^P = 1^-, C = -1, S = +1$ ) found by the LHCb collaboration [1,2]. The results are shown in Fig. 8 for total isospin zero and for three different values of the cutoff used to calculate Eq. (15).

The results are depicted up to the energy corresponding to the three-body threshold for twofold reasons. One is that we are looking for a  $K\rho\bar{D}$  bound state, which can be associated with the  $X_1$  state. Yet other reason is that  $\bar{D}$  and  $\rho$ , recalling the their interaction leads to the formation of  $D_1(2420)$ , as shown in Sec. II, are considered as static or fixed scattering centers. It was shown in Ref. [46] that the results in such a formalism are reliable at energies below the three-body threshold. Discussions on the applicability of the formalism can also be found in Refs. [49,50]. Coming back to the results shown in Fig. 8, it can be said that a bump seems to appear for the value of cutoff 1000 MeV, with the mass  $\sim 3085$  MeV. Such a mass value, however, does not agree with the one determined by LHCb for the  $X_1$  state ( $2904 \pm 5$  MeV).

Let us now look at Fig. 9, which shows the  $K\rho\bar{D}$  amplitude in total isospin 1. Clearly, such a configuration does not form a resonance and only a cusp is seen around the opening of the  $K\bar{D}_1(2420)$  threshold. We can, thus, conclude that neither of the isospin configurations of  $K\bar{D}_1(2420)$  forms a state which can be related to the  $X_1$  state of the LHCb [1,2].

Let us now compare our results with those found in Refs. [24–27]. It is reported in Ref. [24] that the  $K\bar{D}_1(2420)$  system does not bind, neither in the isoscalar

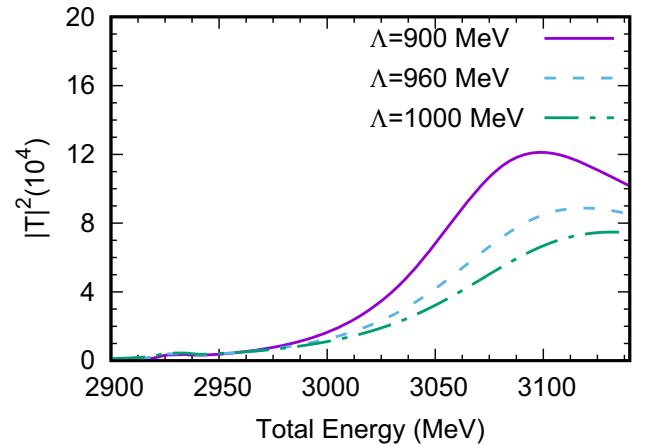


FIG. 8. Modulus squared of the  $T$  matrix for the  $K\rho\bar{D}$  system with total isospin 0.

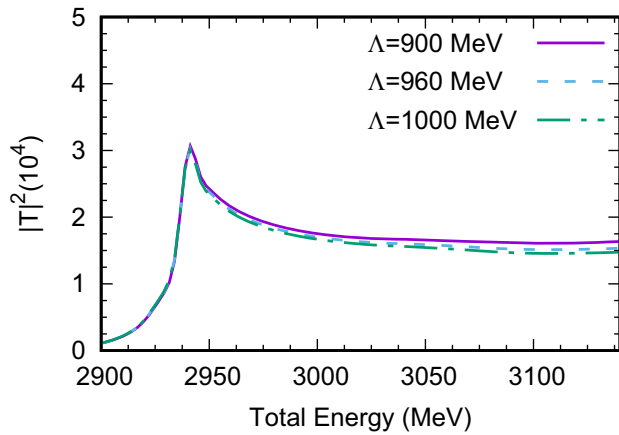


FIG. 9. Modulus squared of the three-body  $T$  matrix for the  $K\rho\bar{D}$  system with total isospin 1.

nor in the isovector configurations. Our results agree with those in Ref. [24]. We find only a bump appearing in the isoscalar  $K\bar{D}_1(2420)$  system above its threshold but below the three-body ( $K\rho\bar{D}$ ) threshold. Recall that Refs. [24–27] treat  $\bar{D}_1(2420)$  as an effective field and study a two-body  $K\bar{D}_1(2420)$  system. We, on the other hand, treat  $\bar{D}_1(2420)$  as a  $\bar{D}\rho$  molecular state and study a three-body system,  $K\rho\bar{D}$ . Our findings also coincide with those in Ref. [25], where only the isoscalar configuration is found to be attractive and requires a very large cutoff to form a bound state. As already stated before, we find a bumplike structure in the isoscalar  $K\bar{D}_1(2420)$  system above its threshold, and not below. Our results, however, do not agree with those in Refs. [26,27]. In Ref. [26], the  $K\bar{D}_1(2420)$  system is found to bind in both isospin configurations, with the binding energy varying in the range  $-5$  to  $-30$  MeV when changing the form factors and cutoff values. The width of the isovector state is found to be narrower ( $\Gamma \sim 12\text{--}30$  MeV) when compared with the isoscalar state ( $\Gamma \sim 60\text{--}100$  MeV). Thus, it is concluded in Ref. [26] that their isoscalar state can be related with  $X_1$ . It is concluded in Ref. [27] too that  $X_1$  can be interpreted as a  $K\bar{D}_1(2420)$  bound state. As discussed above, we do not find the formation of a state below the  $K\bar{D}_1(2420)$  and cannot find a description for the  $X_1$  of Refs. [1,2].

Next we discuss the results obtained for the  $K\rho D$  system. The difference in this case is that all the subsystems interact strongly and lead to formation of a molecular state in one of the two-body isospin configurations. The  $KD$  system forms an isoscalar bound state,  $D_s(2317)$ ;  $K\rho$  and coupled channels generate  $K_1(1270)$ , and as discussed in the previous section,  $D_1(2420)$  can be generated from  $\rho D$  and coupled channel interactions. We show the modulus squared amplitude for the  $K\rho D$  system in total isospin 0 in Fig. 10. A clear peak can be seen with a mass around 2872 MeV and a width of about 100 MeV. The quantum numbers associated with this state are  $I(J^P) = 0(1^-)$  and it

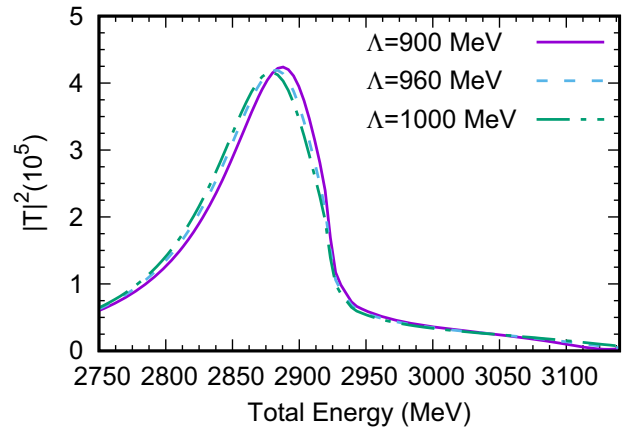


FIG. 10. Modulus squared of the  $T$  matrix for the  $K\rho D$  system with total isospin 0.

has a mass and width in excellent agreement with the known state  $D_{s1}^*(2860)$  [28], with  $M = 2859 \pm 27$  MeV and  $\Gamma = 159 \pm 80$  MeV determined by LHCb [51]. It is important to mention here that the state seen in Fig. 10 has a finite width, even though its mass lies below the three-body threshold. This is so because lighter channels like  $K\pi D_s$  are implicitly present in the system. The presence of such open channels arises through the imaginary part of the two-body  $t$  matrices, which have been calculated in a coupled channel approach. To compare our results with other works, we recall that the  $K_1(1270)D$  and  $KD_1(2420)$  systems were studied separately (uncoupled to each other) in Ref. [24]. The formalism in this former work was built by writing an effective field for the axial mesons and the  $K_1(1270)D$  system was found to form a bound state with mass 3112 MeV, while  $KD_1(2420)$  was found to be weakly attractive. In our case, the three-body system acts simultaneously as  $K_1(1270)D$  and  $KD_1(2420)$  effective systems. Both the systems have similar mass and could be treated as coupled channels in the formalism of Ref. [24]. It sounds plausible that such a treatment could lower the mass of the state found in the  $K_1(1270)D$  system in Ref. [24] since the introduction of a coupled channel usually leads to a more attractive interaction (see Sec. 6 of Ref. [52]).

Finally, we show the modulus squared amplitude for the  $K\rho D$  system with total isospin 1. A narrow and well-pronounced peak is seen in Fig. 11, which is very interesting since the corresponding state must have quantum numbers  $I(J^P) = 1(1^-)$  with charm and strangeness  $+1$ . Such a state cannot be described as a  $q\bar{q}$  state and the higher charged components of the multiplet necessarily require quarks with at least four different flavors in its wave function. The state is, thus, explicitly exotic and would be  $c\bar{s}\bar{q}$ -like partner of the  $\bar{c}\bar{s}qq$ -like  $X_i$  states found by LHCb [1,2]. The state in Fig. 11 has a mass of  $\sim 2883$  MeV and width of  $\sim 7.4 \pm 0.9$  MeV. It can be noticed that though the mass of our  $K\rho D$  isovector state is similar to  $X_i$ s, its width is a lot narrower. In fact it might look

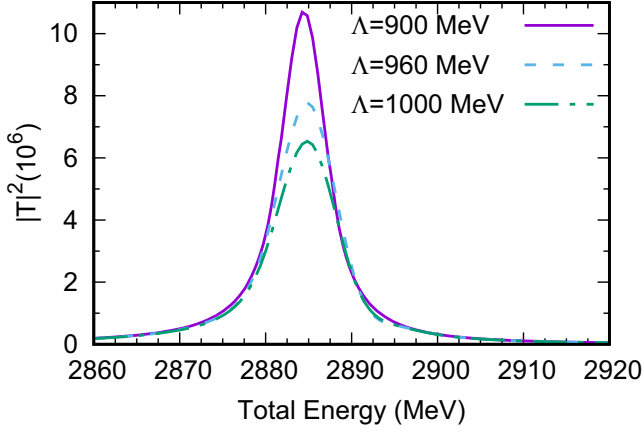


FIG. 11. Modulus squared of the three-body  $T$  matrix for the  $K\rho D$  system with total isospin 1.

surprising that the same system in isospin 0 produces a much wider state. The reason for such a difference is that the isoscalar  $KD$  interaction does not contribute to the three-body interactions with total isospin 0, but does contribute [generating  $D_s(2317)$ ] to the total isospin 1 (see Table II). In other words,  $K\rho D$  with total isospin 1 reorganizes itself, partly, as an effective  $\rho D_s(2317)$  system and the mass of the three-body bound state lies about 200 MeV below the  $\rho D_s(2317)$  threshold. The same system gets contribution from open channels like  $K\pi D_s$  through the imaginary part of the isovector  $DK$  interactions, which produces a finite, though small, width. Such a state has not been found yet and we hope that our findings will encourage its study in future experiments.

#### IV. FURTHER INVESTIGATIONS: $\pi X_i$ INTERACTIONS

Considering that  $X_0$  is proposed to be a  $\bar{K}^* D^*$  molecular state in most works [4–11], we find it useful to investigate if a pion with  $X_0$  can form a bound state. Particularly, we follow Ref. [4] where the  $\bar{K}^* D^*$  system has been found to form isoscalar bound states with  $J^P = 0^+, 1^+$  and  $2^+$ . Our main aim is to test the possibility of the existence of a bound state of pion and the  $1^+$  state of the latter work, since the masses of  $X_i$ s discovered by LHCb differ by less than the mass of a pion.

We, thus, study the three-body system  $\pi \bar{K}^* D^*$ , using the same formalism as presented in the previous section for  $K\rho D$  and  $K\rho \bar{D}$ . In this case we consider  $\bar{K}^* D^*$  to form a cluster and that the pion scatters off its components. Let us denote the three states generated by the  $\bar{K}^* D^*$  interactions in Ref. [4] as  $\tilde{X}_0, \tilde{X}_1$ , and  $\tilde{X}_2$ , where  $\tilde{X}_0$  has  $I(J^P) = 0(0^+)$  with a mass of 2866 MeV and width  $\sim 57$  MeV and which is well identified with the  $X_0$  state of LHCb. The other states,  $\tilde{X}_1$  has  $I(J^P) = 0(1^+)$ , a mass of 2861 MeV and about 20 MeV of width, and  $\tilde{X}_2$  has  $I(J^P) = 0(2^+)$ , a mass of 2775 MeV and a width of 38 MeV. We study the three

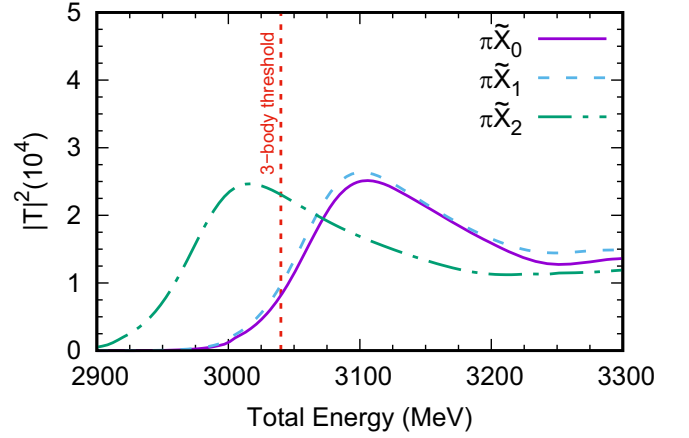


FIG. 12. Modulus squared of the three-body  $T$  matrix for the  $\pi \bar{K}^* D^*$  system considering  $\bar{K}^* D^*$  to cluster as  $\tilde{X}_0, \tilde{X}_1$ , and  $\tilde{X}_2$  of Ref. [4].

possible configurations of  $\pi \bar{K}^* D^*$ :  $\pi \tilde{X}_0, \pi \tilde{X}_1$ , and  $\pi \tilde{X}_2$ . All the three system have total isospin 1, since the  $\bar{K}^* D^*$  subsystem clusters with total isospin 0, and have the spin parity  $0^-, 1^-,$  and  $2^-$ , respectively.

Considering the findings of Ref. [4] to describe the cluster and determining the amplitudes for the  $\pi \bar{K}^*, \pi D^*$  subsystems by solving the Bethe-Salpeter equation following Refs. [30,41], we determine the three-body  $T$  matrix. We must emphasize that the amplitude for  $\pi D^*$  is obtained by considering  $D\rho$  and other coupled channels, by including the box diagrams, as described in Sec. II. The coupled channel system generates  $D_1(2420)$  though, as mentioned in Sec. II, it couples weakly to  $\pi D^*$ . Similarly,  $\pi \bar{K}^*$  is a coupled channel of  $K\rho$  and other pseudoscalar-vector meson systems that generate  $K_1(1270)$ .

We present the modulus squared three-body amplitudes in Fig. 12 for the three possible total spins of the system. As can be seen, a three-body bound state with mass around 2900 MeV is not found in the  $\pi \bar{K}^* D^*$  system with isospin 1. The  $\pi \tilde{X}_2$  amplitude is seen to increase with the energy, indicating that a state may get formed at higher energies. We have extended our calculations to higher energies and find that a very wide bump-like structure appears in the squared amplitude at energies above the three-body threshold. We would, however, not make any claims since the calculations above the three-body threshold may not be reliable with our present formalism.

We can conclude this section by mentioning that the  $X_1$  of LHCb cannot be described as  $\pi \bar{K}^* D^*$  bound state.

#### V. SUMMARY AND FUTURE PERSPECTIVES

In the present work we have investigated the possibility of describing the  $X_1(2900)$  found by LHCb [1,2] as a molecular state of  $K\rho \bar{D}$  or  $\pi \bar{K}^* D^*$ . We first argue that the  $D\rho$  interaction is strongly related to  $D_1(2420)$  as first

proposed in Ref. [30]. We update this former work by including box diagrams with a pseudoscalar exchange and by adjusting the model parameters to obtain the properties of  $D_1(2420)$  in better agreement with the latest data. We then study three-body systems by treating  $D\rho$  ( $\bar{D}\rho$ ) as components of  $D_1(2420)$ , which remain static in the scattering. Within such an approximation, we find that the  $K\rho\bar{D}$  system could form a wide state but with a mass higher than that of the  $X_1$  state found by LHCb [1,2]. We, thus, conclude that  $X_1$  must have a description different than a  $K\rho\bar{D}$  molecule.

Taking the advantage of the symmetry between  $\bar{D}\rho$  and  $D\rho$  interactions, we study the  $K\rho D$  system. In this case, we find that the system generates states in the total isospin 0 as well as 1 configurations. The properties of the isoscalar state turn out to be in excellent agreement with those of  $D_{s1}^*(2860)$  [28], implying that it can be understood as a three-body molecular resonance. The isovector state is clearly exotic, requiring more than two quarks for its description. This latter state is narrow, having a width less than 10 MeV, and a mass similar to that of the  $X_1$ s found by LHCb.

In the case of  $\pi\bar{K}^*D^*$ , we follow Ref. [4] where  $\bar{K}^*D^*$  interactions have been studied thoroughly, providing a molecular description for  $X_0(2900)$  [1,2], and proposing the existence of two other states with spin parity  $1^+$ ,  $2^+$ . The investigations have been further extended in Refs. [53,54] suggesting reactions to observe the new predicted states. Treating  $\bar{K}^*D^*$  as states with three possible  $J^P$  values, as found in Ref. [4], we study the  $\pi\bar{K}^*D^*$  interaction. We do not find a state which can be associated with  $X_1$ , although bump

like structures are found at energies around 3000–3100 MeV. Such bumps lie in the energy region beyond the applicability of the FCA and a more detailed study would be necessary to make more robust claims.

As future perspectives of the current study, it should be useful to investigate further the properties of the states found in this work. For example, it can be worthwhile to determine the decay rates of the  $K\rho D$  and  $K\rho\bar{D}$  states, with isospin 0, to different possible final states. The former state is associated with  $D_{s1}^*(2860)$  in our work, for which not much is known on its decay properties. A theoretical study of such properties can be helpful in experimental investigations of the properties of  $D_{s1}^*(2860)$ .

## ACKNOWLEDGMENTS

B. B. M., K. P. K., and A. M. T. gratefully acknowledge the support from the Fundação de Amparo à Pesquisa do Estado de São Paulo (FAPESP), Grants No. 2020/00676-8, No. 2019/17149-3, and No. 2019/16924-3. K. P. K. and A. M. T. are also thankful to the Conselho Nacional de Desenvolvimento Científico e Tecnológico (CNPq) for Grants No. 305526/2019-7 and No. 303945/2019-2. This work is partly supported by the Spanish Ministerio de Economía y Competitividad and European FEDER funds under Contract No. PID2020–112777 GBI00, and by Generalitat Valenciana under Contract No. PROMETEO/2020/023. This project has received funding from the European Unions 10 Horizon 2020 research and innovation programme under Grant Agreement No. 824093 for the “STRONG-2020” project.

- 
- [1] R. Aaij *et al.* (LHCb Collaboration), *Phys. Rev. Lett.* **125**, 242001 (2020).
  - [2] R. Aaij *et al.* (LHCb Collaboration), *Phys. Rev. D* **102**, 112003 (2020).
  - [3] R. Molina, T. Branz, and E. Oset, *Phys. Rev. D* **82**, 014010 (2010).
  - [4] R. Molina and E. Oset, *Phys. Lett. B* **811**, 135870 (2020).
  - [5] M. Z. Liu, J. J. Xie, and L. S. Geng, *Phys. Rev. D* **102**, 091502 (2020).
  - [6] H. X. Chen, W. Chen, R. R. Dong, and N. Su, *Chin. Phys. Lett.* **37**, 101201 (2020).
  - [7] Y. Huang, J. X. Lu, J. J. Xie, and L. S. Geng, *Eur. Phys. J. C* **80**, 973 (2020).
  - [8] M. W. Hu, X. Y. Lao, P. Ling, and Q. Wang, *Chin. Phys. C* **45**, 021003 (2021).
  - [9] S. S. Agaev, K. Azizi, and H. Sundu, *J. Phys. G* **48**, 085012 (2021).
  - [10] H. X. Chen, *Phys. Rev. D* **105**, 094003 (2022).
  - [11] S. Y. Kong, J. T. Zhu, D. Song, and J. He, *Phys. Rev. D* **104**, 094012 (2021).
  - [12] M. Karliner and J. L. Rosner, *Phys. Rev. D* **102**, 094016 (2020).
  - [13] X. G. He, W. Wang, and R. Zhu, *Eur. Phys. J. C* **80**, 1026 (2020).
  - [14] Z. G. Wang, *Int. J. Mod. Phys. A* **35**, 2050187 (2020).
  - [15] J. R. Zhang, *Phys. Rev. D* **103**, 054019 (2021).
  - [16] G. J. Wang, L. Meng, L. Y. Xiao, M. Oka, and S. L. Zhu, *Eur. Phys. J. C* **81**, 188 (2021).
  - [17] S. S. Agaev, K. Azizi, and H. Sundu, *Nucl. Phys.* **A1011**, 122202 (2021).
  - [18] Q. F. Lü, D. Y. Chen, and Y. B. Dong, *Phys. Rev. D* **102**, 074021 (2020).
  - [19] R. M. Albuquerque, S. Narison, D. Rabetiarivony, and G. Randriamanatrika, *Nucl. Phys.* **A1007**, 122113 (2021).
  - [20] X. H. Liu, M. J. Yan, H. W. Ke, G. Li, and J. J. Xie, *Eur. Phys. J. C* **80**, 1178 (2020).

- [21] T. J. Burns and E. S. Swanson, *Phys. Rev. D* **103**, 014004 (2021).
- [22] Y. K. Chen, J. J. Han, Q. F. Lü, J. P. Wang, and F. S. Yu, *Eur. Phys. J. C* **81**, 71 (2021).
- [23] F. S. Yu, *Eur. Phys. J. C* **82**, 641 (2022).
- [24] X. K. Dong and B. S. Zou, *Eur. Phys. J. A* **57**, 139 (2021).
- [25] J. He and D. Y. Chen, *Chin. Phys. C* **45**, 063102 (2021).
- [26] J. J. Qi, Z. Y. Wang, Z. F. Zhang, and X. H. Guo, *Eur. Phys. J. C* **81**, 639 (2021).
- [27] H. Chen, H. R. Qi, and H. Q. Zheng, *Eur. Phys. J. C* **81**, 812 (2021).
- [28] R. L. Workman *et al.* (Particle Data Group), *Prog. Theor. Exp. Phys.* **2022**, 083C01 (2022).
- [29] W. I. Eshraim, F. Giacosa, and D. H. Rischke, *Eur. Phys. J. A* **51**, 112 (2015).
- [30] D. Gamermann and E. Oset, *Eur. Phys. J. A* **33**, 119 (2007).
- [31] F. Aceti, M. Bayar, E. Oset, A. Martínez Torres, K. P. Khemchandani, J. M. Dias, F. S. Navarra, and M. Nielsen, *Phys. Rev. D* **90**, 016003 (2014).
- [32] M. Bando, T. Kugo, and K. Yamawaki, *Phys. Rep.* **164**, 217 (1988).
- [33] W. H. Liang, C. W. Xiao, and E. Oset, *Phys. Rev. D* **89**, 054023 (2014).
- [34] R. Aaij *et al.* (LHCb Collaboration), *Phys. Rev. D* **101**, 032005 (2020).
- [35] M. Ablikim *et al.* (BESIII Collaboration), *Phys. Lett. B* **804**, 135395 (2020).
- [36] K. A. Brueckner, *Phys. Rev.* **90**, 715 (1953).
- [37] R. C. Barrett and A. Deloff, *Phys. Rev. C* **60**, 025201 (1999).
- [38] S. S. Kamalov, E. Oset, and A. Ramos, *Nucl. Phys.* **A690**, 494 (2001).
- [39] A. Martínez Torres, K. P. Khemchandani, L. Roca, and E. Oset, *Few Body Syst.* **61**, 35 (2020).
- [40] L. Roca, E. Oset, and J. Singh, *Phys. Rev. D* **72**, 014002 (2005).
- [41] L. S. Geng, E. Oset, L. Roca, and J. A. Oller, *Phys. Rev. D* **75**, 014017 (2007).
- [42] F. K. Guo, P. N. Shen, H. C. Chiang, R. G. Ping, and B. S. Zou, *Phys. Lett. B* **641**, 278 (2006).
- [43] A. Martínez Torres, E. Oset, S. Prelovsek, and A. Ramos, *J. High Energy Phys.* **05** (2015) 153.
- [44] A. Martínez Torres, E. Oset, S. Prelovsek, and A. Ramos, *Proc. Sci. Hadron2017* (**2018**) 024.
- [45] A. Martínez Torres, L. R. Dai, C. Koren, D. Jido, and E. Oset, *Phys. Rev. D* **85**, 014027 (2012).
- [46] A. Martínez Torres, E. J. Garzon, E. Oset, and L. R. Dai, *Phys. Rev. D* **83**, 116002 (2011).
- [47] L. Roca and E. Oset, *Phys. Rev. D* **82**, 054013 (2010).
- [48] X. L. Ren, B. B. Malabarba, L. S. Geng, K. P. Khemchandani, and A. Martínez Torres, *Phys. Lett. B* **785**, 112 (2018).
- [49] J. J. Xie, A. Martínez Torres, and E. Oset, *Phys. Rev. C* **83**, 065207 (2011).
- [50] B. B. Malabarba, K. P. Khemchandani, and A. M. Torres, *Eur. Phys. J. A* **58**, 33 (2022).
- [51] R. Aaij *et al.* (LHCb Collaboration), *Phys. Rev. Lett.* **113**, 162001 (2014).
- [52] F. Aceti, L. R. Dai, L. S. Geng, E. Oset, and Y. Zhang, *Eur. Phys. J. A* **50**, 57 (2014).
- [53] L. R. Dai, R. Molina, and E. Oset, *Phys. Lett. B* **832**, 137219 (2022).
- [54] L. R. Dai, R. Molina, and E. Oset, *Phys. Rev. D* **105**, 096022 (2022).